scientific reports

Check for updates

OPEN

Impact of some inorganic anions on the corrosion of nickel in a solution containing Na_2SO_4 and $NaClO_4$

M. A. Deyab[1]✉, Majed M. Alghamdi[2] & Adel A. El-Zahhar[2]

Potentiodynamic study was carried out on nickel in Na_2SO_4 solution in the presence of ClO_4^-, WO_4^{2-}, MoO_4^{2-}, NO_2^- and NO_3^- ions. The anodic excursion spans of the metal nickel in a solution of Na_2SO_4 are marked by the appearance of clearly defined anodic peak, passive region, and transpassive shoulder. According to the data, the anodic peak current density (I_{PAI}) rise from 1.82 to 8.12 mA cm^{-2} as the concentration of the Na_2SO_4 solution rises from 0.2 to 1.0 M. It is clear that as scan rate increases, the I_{PAI} rises reaching to 11.8 mA cm^{-2}. The apparent activation energy of nickel corrosion in Na_2SO_4 is 33.25 kJ mol^{-1}. ClO_4^- anion addition speeds up nickel's active dissolution, as well tends to break down the passive layer, and causes pitting penetration. It was found that, the pitting potential (E_{pit}) of nickel in solutions containing the two anions ClO_4^- and SO_4^{2-} shifts to the positive direction by addition of WO_4^{2-}, MoO_4^{2-}, NO_2^- anions and shifts to the negative direction by addition NO_3^- anion. E_{pit} increased by 0.67, 0.37 and 0.15 V in the presence of WO_4^{2-}, MoO_4^{2-} and NO_2^-, respectively. $WO_4^{2-} > MoO_4^{2-} > NO_2^-$ was the order in which the inhibitors were most effective.

Nickel has attracted many investigations of its electrochemical and other properties in different electrolytes[1–4], due to its wide speared industrial applications. Nickel is a metal with strong resistance to corrosion according to many circumstances; however, it may still corrode under some conditions. Nickel corrosion behavior is affected by environmental variables, including the existence of corrosive chemicals, and the specific type of nickel (for instance, native nickel, nickel alloys).

Nickel may corrode in corrosive conditions, especially those including halides e.g. chlorides. The incorporation of halides can hasten the corrosion process by breakdown the passivity of the nickel surface[5–7]. The proposed mechanisms in which chlorides ions are adsorbed on the nickel surface in competition with water molecules as the following:

$$Ni + H_2O \rightarrow Ni(H_2O)_{ads}, \quad (1)$$

$$Ni + Cl^- \rightarrow Ni\left(Cl^-\right)_{ads}, \quad (2)$$

$$Ni\left(Cl^-\right)_{ads} \rightarrow NiCl + e^-, \quad (3)$$

$$NiCl + Cl^- \rightarrow NiCl_{2(aq.)} + e^-. \quad (4)$$

In the presence of other different species, including perchlorate, sulphate, and nitrate ions, localized corrosion of nickel can also happen[8]. Several corrosion preventative methods can be used to reduce nickel corrosion that includes:

Coatings: Using protection coatings like nickel plating, electroless metal coatings, as well as organic coatings might give an extra shield towards corrosion[9].

Alloying: To improve corrosion resistance in certain settings, the alloy of nickel with additional elements can be used. Because of their superior resistance to different corrosive chemicals, nickel-based alloys such as Inconel or Hastelloy alloy are frequently used in corrosive settings[10].

[1]Egyptian Petroleum Research Institute, Nasr City 11727, Cairo, Egypt. [2]Department of Chemistry, college of Science, King Khalid University, P.O. Box 9004, 61413 Abha, Saudi Arabia. ✉email: hamadadeiab@yahoo.com

Cathodic protection: Using cathodic protection methods including sacrificial electrodes system or impressed current structures, nickel may be protected from corrosion[11].

Nickel corrosion resistance may be significantly improved by chromate ions[12,13]. Chromate is first adsorbed on the cathodic sites of the metal surface, followed by electrochemical cathodic reduction to give some kinds of Cr oxides. This oxide layer acts as a barrier from further corrosion by blocking corrosive substances such as oxygen and moisture from accessing the underlying metal. By encouraging the creation of a stable and protective chromium oxide layer, the chromate ion passivation technique can improve the corrosion resistance of nickel. In alkaline or somewhat acidic situations, chromate passivation is especially effective. But as a result to their toxicity, hexavalent chromium material, such as chromate ions have recently caused environmental issues. As a consequence, studies regarding new, environmentally conscious corrosion inhibitors and passivation approaches have changed.

In the current work, alternative inorganic materials, WO_4^{2-}, MoO_4^{2-}, NO_2^-, NO_3^- ions are being explored for their anti-corrosion properties on nickel in Na_2SO_4 solution in the presence of perchlorate ions. These ions are considered as a less toxic alternative to hexavalent chromium compounds. Ongoing research aims to optimize the use of these inorganic materials and develop effective passivation materials for nickel and its alloys.

Experimental

Polarization measurements were performed on cylindrical electrodes machined nickel rod (99.98%, surface area 0.463 cm^{-2}). Every time, the nickel surface was cleaned up by using emery paper for polishing from no. 400 to no. 2500. Finally, the working electrode was washed with double distilled water and degreased with acetone. Studies on potentiodynamic polarization were conducted using a computer and a potentiostat instrument (Gamry-3000). The tests have been carried out in a standard three-compartment cell employing a saturated calomel electrode to be the reference electrode, a platinum foil to be the auxiliary electrode, and nickel to be the working electrode. The polarization curves were swept from − 2.0 to 2.0 V. Potential scan rate range from 20 to 100 mV s^{-1}.

Chemicals of analytical grade and three-time distilled pure water were used to create solutions. For all studies, various concentrations of Na_2SO_4 solutions were prepared using laboratory-grade Na_2SO_4 (Merck) and triple distilled water. Sigma-Aldrich Company supplied the inorganic compounds ($NaClO_4$, Na_2WO_4, $NaNO_2$, $NaNO_3$), which were utilized without any extra purification. By submerging the cell in a water thermostat, the temperature of the experiment's solution was regulated with a temperature range of 30–70 °C. All experiments were conducted in aerated solutions.

The surface morphology of some samples after immersion for 120 h at 30 °C was performed using Scanning Electron Microscope (SEM) ZEISS Gemini-SEM Microscopy.

Results and discussion

Electrochemical polarization of nickel in Na_2SO_4 solution

Typical polarization curves of nickel in various concentrations of Na_2SO_4 solution (0.2 to 1.0 M) are given in Fig. 1. The curves were swept from -2.0 V to 2.0 V at scan rate $\upsilon = 20$ mVs^{-1} and at 30 °C. On positive going scan, the cathodic current density decreases continually reaching corrosion potential (E_{corr}) at zero current density. Prior to the oxygen evolution reaction, each anodic curve shows one dissolution peak (I), a definitive passive

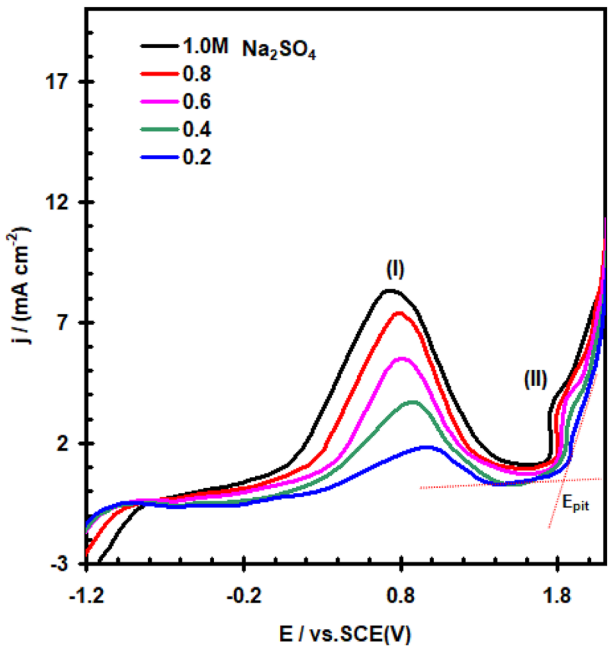

Figure 1. Polarization curve for nickel electrode in Na_2SO_4 solution at 30 °C with scan rate of 20 mVs^{-1}.

state, and a transpassive state (II). The dissolution peak (I) of nickel is related to electroformation of hydrous $Ni(OH)_2$[14–16] layer, which is transformed chemically and electrochemically to produce the passive NiO layer in the end[17–19]. When the concentration of nickel oxide exceeds the solubility product of NiO, precipitation of a porous oxide film occurs on the electrode surface. The current decreases to an extremely low value, signalling the beginning of primary passivation, when the surface is completely covered with a nonporous passive film. The passivation current start to increase markedly, forming transpassive state prior to oxygen evaluation. Sato and Kamoto[20–23] attributed this behaviour to the dissolution of Nickel yielding Ni^{2+} ions, through active spots in the passive film.

The anodic peak current density (I_{PA1}) rise from 1.82 to 8.12 mA cm^{-2} as the concentration of the Na_2SO_4 solution rises from 0.2 to 1.0 M, as shown in Fig. 1. Furthermore, as the concentration of the Na_2SO_4 solution increases, the anodic peak potential relatively shifts in a less positive direction.

Figure 2 depicts the findings of this study on the effect of potential scan rate (υ) on the potentiodynamic polarization of a nickel electrode in 0.4 M Na_2SO_4 solution at 30 °C. It is clear that as υ increases, the peak current density (I_{PA1}) rises reaching to 11.8 mA cm^{-2} and its peak potential (E_{PA1}) moves towards more negative values. Good linearity of the (I_{PA1}) verses $\upsilon^{1/2}$ plot was observed (Fig. 3), but do not pass through the origin. It illustrates that a combined operation including direct film formation and diffusion-controlled dissolve may be used to explain the oxide layer formation process in the potential area of peak A1.

Figure 4 shows the effect of solution temperature on the potentiodynamic polarization response of nickel in 0.4 M Na_2SO_4 solution at scan rate of 20 mVs^{-1}. The data clearly show that, the rise of temperature increases the value of I_{PA1} and slightly shifts its peak potential towords more negative values. This is results can be interpreted on the bases of the fact that, at high temperature, porous oxide film is then, soft, and non-protective. This is

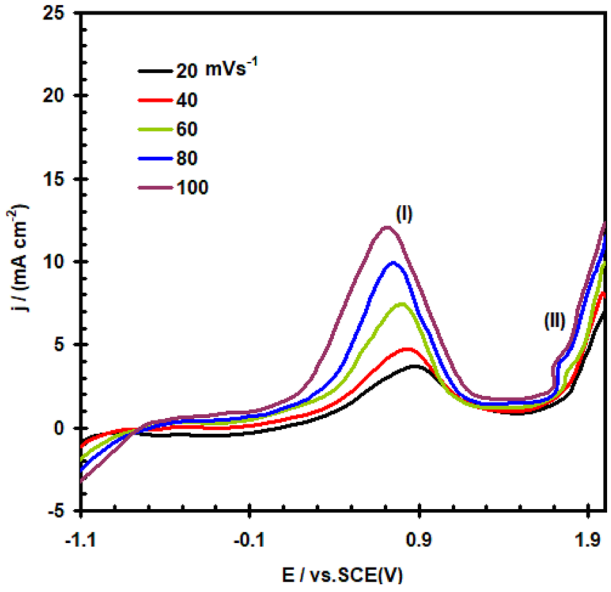

Figure 2. Polarization curve for nickel electrode in 0.4 M of Na_2SO_4 solution at 30 °C at different scan rate.

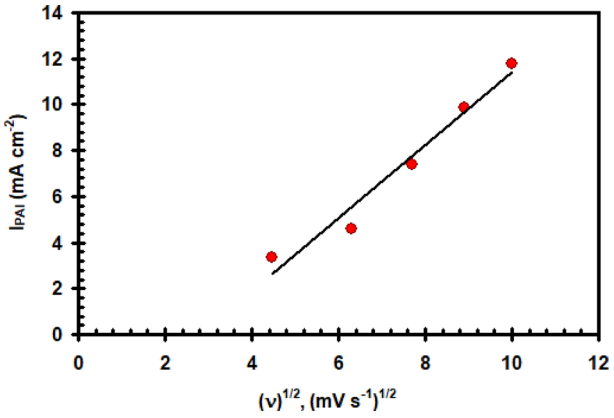

Figure 3. Relation between (I_{PAI}) vs. the square root of scan rate for nickel electrode in 0.4 M of Na_2SO_4 solution at 30 °C.

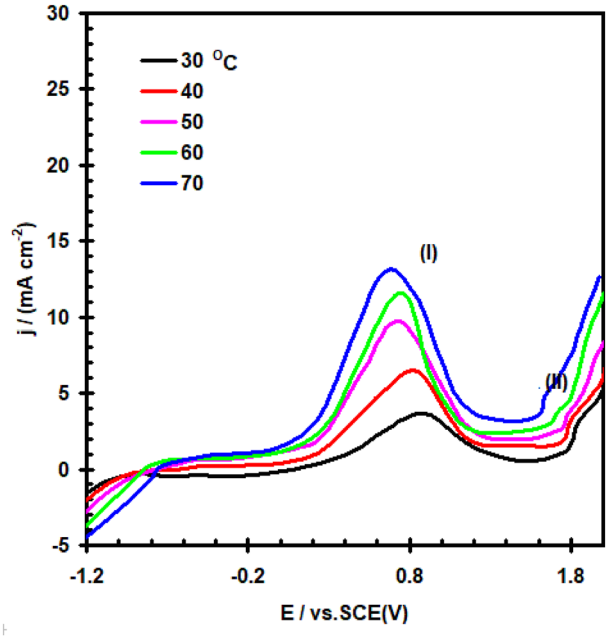

Figure 4. Polarization curve for nickel electrode in 0.4 M of Na_2SO_4 solution with scan rate of 20 mVs^{-1} at different temperatures.

because, the solubility of the oxide film by the electrolyte increase with increasing temperature, thus enhancing the anodic dissolution processes[24]. Rise in temperature in temperature also accelerates the transport of reagent and reaction products to and from electrode surface[25].

In Fig. 5, the values of log I_{PA1} are displayed as variables of (1/T)(K) (Arrhenius graph) for several temperatures. Based on the slope of that Arrhenius plotting, the apparent activation energy E_a for anodic reaction was determined. The data provide a value for the apparent activation energy, $E_a = 33.25$ kJ mol^{-1}.

Effect ClO_4^- ions on the electrochmeical behavior of nickel

It was investigated how different $NaClO_4$ addition concentrations (0.1–0.5 M) affected the potentiodynamic, E/I, polarization of nickel in 0.4 M Na_2SO_4 at 30 °C and 20 mVs^{-1} scan rate (see Fig. 6). The data shows that, the progressive additions of $NaClO_4$ cause an increase in the peak current density (I_{PA}) of the anodic peaks and shifts its potential to more negative. These findings imply that perchlorate ions disrupt the oxidation operations of nickel electrodes. Competing with SO_4^{2-} ions for adsorption on the bare metal surface, ClO_4^- ions can take part in electrode dissolution processes directly[26]. However, the ClO_4^- in the sulphate liquid increases I_{pass} and has a tendency to dissolve the passive layer. The passive current goes up abruptly and strongly at a specific critical potential (E_{pit}), signifying the breakdown of the passive barrier and the beginning and progression of the pitting.

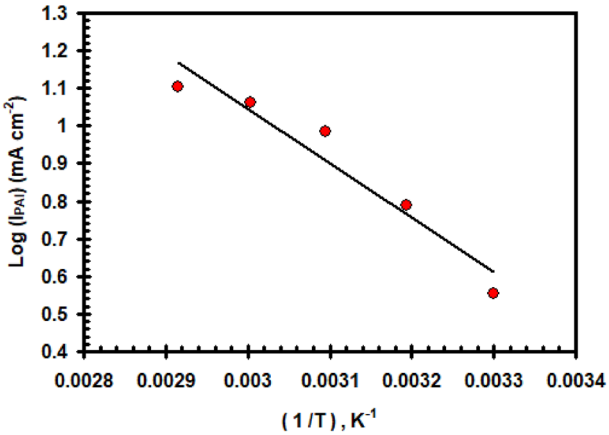

Figure 5. Relation between log (I_{PAI}) vs. (1/T) for nickel electrode in 0.4 M of Na_2SO_4 solution with scan rate of 20 mVs^{-1}.

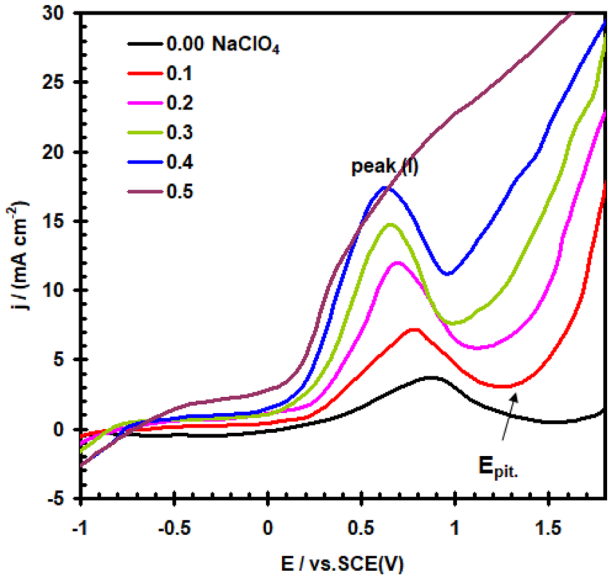

Figure 6. Effect of addition ClO_4^- ion on the potentiodynamic polarization curve for nickel electrode in 0.4 M of Na_2SO_4 solution with scan rate of 20 mVs^{-1} at 30 °C.

As the amount of ClO_4^- gets higher, the pitting potential (E_{pit}) moves to an increasingly negative (active) location. Figure 7 data demonstrates that, in accordance with Eq. (5), E_{pit} is in a linear manner linked to log [ClO_4^-].

$$E_{pit} = x - y \log\left(ClO_4^-\right), \tag{5}$$

where x and y are constants and depends on the condations and nature of the electrode.

The adsorption of ClO_4^- on the oxide wrapped layer, specifically at its weakness points and flaws, can be attributed to the breakdown of the definitive passive barrier and the beginning of the pitting corrosion. Pit growth begins earlier when ClO_4^- concentration increases due to its mobility and acidity increases as a result of metal cation hydrolysis within pits[27].

In Fig. 8, the significance of the scan rate (υ) regarding the E/I relation of a nickel electrode in a 0.4 M solution of Na_2SO_4 containing 0.3 M $NaClO_4$ are shown. The anodic peak current is enhanced and has a more negative peak potential as υ increases. Furthermore, the increase in υ shifts E_{pit} towards a more positive value. Incubation time is used to clarify this attitudes[28]. Once the scan has become high, pitting beginning takes place at higher positive potentials, which relate to a short enough incubation period—that is, the period of time required to penetrate the passive layering system.

Plotting I_{PA} vs. $\upsilon^{1/2}$ yielded a linear trend depicted in Fig. 9.The resulting straightaway fails to pass through the origin. In theory, the plotting I_{PA} vs. $\upsilon^{1/2}$ shows that diffusion is partially controlling the anodic dissolution operations on nickel in the existence of ClO_4^- anion[29].

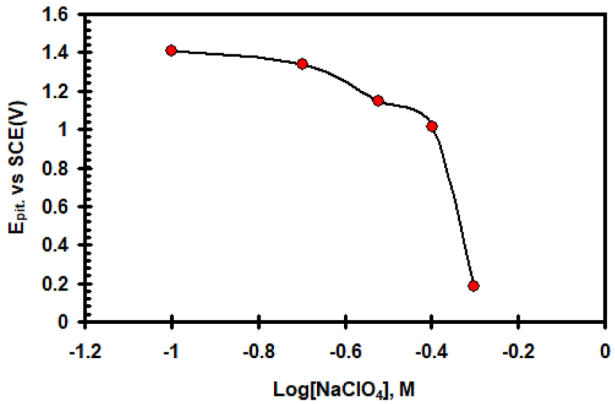

Figure 7. Relation between (E_{pit}) vs. log [ClO_4^-] for nickel electrode in 0.4 M of Na_2SO_4 solution with scan rate of 20 mVs^{-1} at 30 °C.

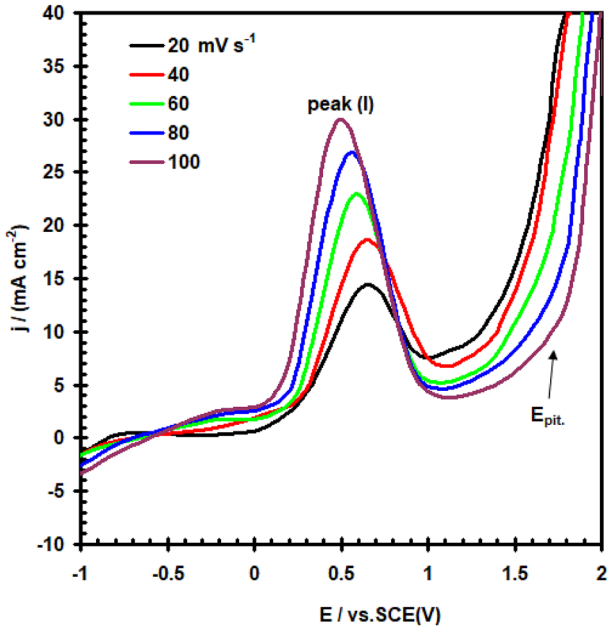

Figure 8. Potentiodynamic polarization curve for nickel electrode in (0.4 M Na_2SO_4 + 0.3 M ClO_4^-) solution at 30 °C at different scan rate.

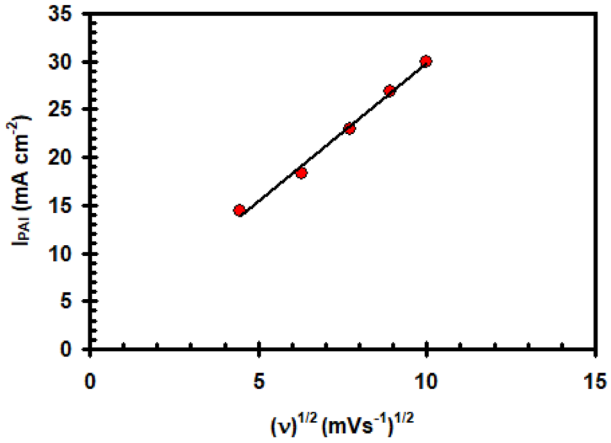

Figure 9. Relation between (I_{PAI}) vs. the square root of scan rate for nickel electrode in (0.4 M Na_2SO_4 + 0.3 M ClO_4^-) solution at 30 °C.

Effect of added inorganic anions on pitting corrosion

The impact of WO_4^{2-}, MoO_4^{2-}, NO_2^- and NO_3^- ions as corrosion-inhibiting agents has been investigated with the goal to learn more concerning the particular function that certain inorganic inhibitors serve on the preventing corrosion mechanisms taking place between the interface between the pure nickel electrode and the electrolyte. E/I curves for nickel in a solution of (0.4 M $NaSO_4$ + 0.3 M $NaClO_4$) at 30 °C are shown in Figs. 10 and 11, which show the effects when adding different amounts of WO_4^{2-} and NO_3^- anions in turn. Figure 12 depicts the dependent relationship of E_{pit} on logarithmic inorganic salts concentration.

Analyses of data in Figs. 10, 11, 12 show that, based on the kind and amount of the inhibitor, the existence of all of these anions (except NO_3^-), hinders the overall corrosion of nickel to a particular extent. The decline in I_{PA} and the positive departure of the E_{pit} demonstrate this clearly (see Tables 1 and 2). It is evident that these agents have a decreasing effect on nickel's active dissolution in the following order: $WO_4^{2-} > MoO_4^{2-} > NO_2^-$. The adsorption competition of the inhibitor SO_4^{2-} and ClO_4^- ions on the the outermost layer of the electrode is thought to hinder corrosion. Adsorption and founding of SO_4^{2-} and ClO_4^- are hindered by the adsorption inhibitor ions. As a result, the SO_4^{2-} and ClO_4^- anions'surface coverage diminished by the adsorbed inhibitor ions, and the total number of areas of defect at the film's surface that the anions could enter was also decreased. The difference of the molar polarisation of these ions, which is in the order $WO_4^{2-} > MoO_4^{2-} > NO_2^-$, may be responsible for the

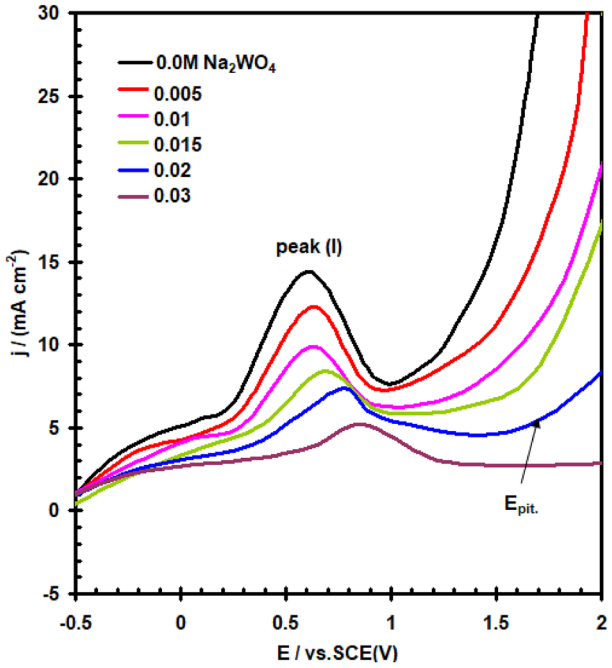

Figure 10. Effect of addition WO_4^{2-} ions on the potentiodynamic polarization curve for nickel electrode in (0.4 M Na_2SO_4 + 0.3 M ClO_4^-) solution with scan rate of 20 mVs^{-1} at 30 °C.

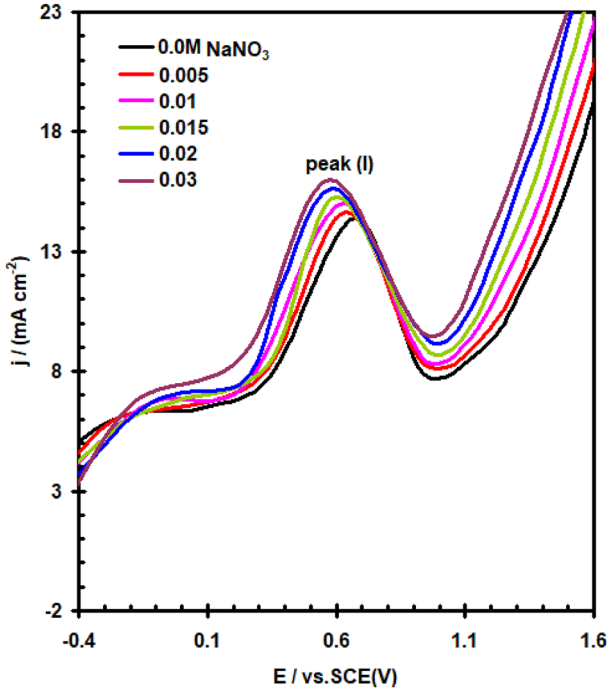

Figure 11. Effect of addition NO_3^- ions on the potentiodynamic polarization curve for nickel electrode in (0.4 M Na_2SO_4 + 0.3 M ClO_4^-) solution with scan rate of 20 mVs^{-1} at 30 °C.

different anions' inhibitory properties[30]. Because anion molar polarisation is believed to be entirely correlated to ions adsorption[31], the inhibitory impact should improve with enhancing ions adsorption over the electrode. Surface active ions with higher defarmability are likely to adsorb onto the nickel surface, reducing the actual area that can be used by redox ions for reaction. Figure 11 data show that the NO_3^- anion promotes the I_{PAI} and moves the $E_{pit.}$ in a negative way. These impacts may be clarified by the NO_3^- anion's lower polarizability value with respect to the severe SO_4^{2-} and ClO_4^- ions[32].

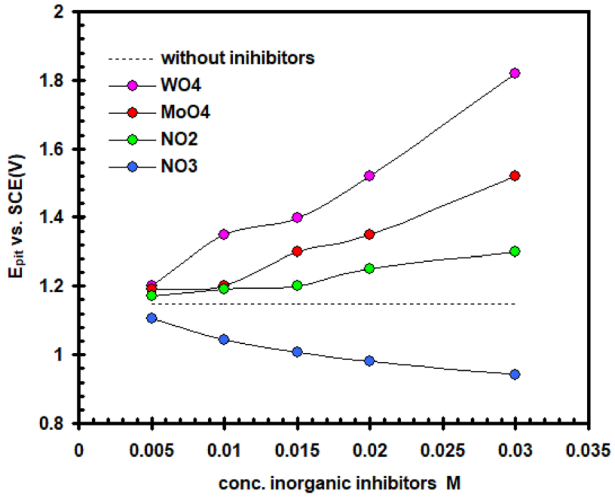

Figure 12. Relationship between (E_{pit}) and inorganic inhibitors concentrations for nickel in a solution containing 0.4 M Na_2SO_4 and 0.3 M ClO_4^-.

Inorganic inhibitors conc. M	Blank solution (0.4 M Na_2SO_4 + 0.3 M ClO_4^-) E_{pit} V(SCE)	E_{pit} V(SCE)			
		WO_4^{2-}	MoO_4^{2-}	NO_2^-	NO_3^-
0	1.15	–	–	–	–
0.005	–	1.20	1.19	1.17	1.11
0.01	–	1.35	1.20	1.19	1.04
0.015	–	1.40	1.30	1.20	1.01
0.02	–	1.52	1.35	1.25	0.98
0.03	–	1.82	1.52	1.30	0.94

Table 1. The pitting potential (E_{pit}) for nickel electrode in (0.4 M Na_2SO_4 + 0.3 M ClO_4^-) solution in the absence and presence of amounts of WO_4^{2-}, MoO_4^{2-}, NO_2^- and NO_3^- anions.

Inorganic inhibitors conc. M	Blank solution (0.4 M Na_2SO_4 + 0.3 M ClO_4^-) I_{PAI} mA cm^{-2}	I_{PAI} mA cm^{-2}			
		WO_4^{2-}	MoO_4^{2-}	NO_2^-	NO_3^-
0	14.4	–	–	–	–
0.005	–	12.3	13.11	13.51	14.66
0.01	–	9.89	11.82	12.58	15.00
0.015	–	8.39	9.53	11.33	15.25
0.02	–	7.36	8.17	10.89	15.58
0.03	–	5.21	7.24	9.94	16.00

Table 2. The anodic peak current density (I_{PA1}) for nickel electrode in (0.4 M Na_2SO_4 + 0.3 M ClO_4^-) solution in the absence and presence of amounts of WO_4^{2-}, MoO_4^{2-}, NO_2^- and NO_3^- anions.

The amount of inorganic salts needed to produce a significant positive shift in E_{pit} (as indicated inhibition) improves in the following sequence: $NO_2^- > MoO_4^{2-} > WO_4^{2-}$ (see Fig. 12). Because of their particular adsorbility,

Inorganic inhibitors conc. M	*IE*%		
	WO_4^{2-}	MoO_4^{2-}	NO_2^-
0.005	14.5	8.9	6.1
0.01	31.3	17.9	12.6
0.015	41.7	33.8	21.3
0.02	48.8	43.2	24.3
0.03	63.8	49.7	39.9

Table 3. The corrosion inhibition efficiency of inorganic inhibitors for nickel in (0.4 M Na_2SO_4 + 0.3 M ClO_4^-) solution.

these inhibitors are able to remove ClO_4^- ion from the locations where it more readily enters the passive coating, which improves pitting resistance against corrosion[33,34].

Furthermore, the reduced modes of these inhibitors (WO_2 and MoO_2), for example, transform into component of the passivating oxide and have a tendency to block its pores and weaknesses getting more effectively shielding capabilities. on the additional one, nitrite ions had been found to be reduced to ammonia in which oxygen that remained on the surface triggered the oxide reaction[35]. Figure 12 data demonstrate that the incorporation of NO_3^- ions moves E_{pit} to a more negative direction, demonstrating that NO_3^- ions encourage pitting corrosion. The finding could be explained by the relatively low polarizability of NO_3^- ions[36] in comparison to other ions.

The inhibition corrosion efficiency (*IE*%) of various inorganic ions was estimated as follows[37]:

$$\mathrm{IE}\,\% = \frac{\mathrm{I_{PA(0)}} - \mathrm{I_{PA}}}{\mathrm{I_{PA(0)}}} \times 100, \tag{6}$$

where $I_{PA(0)}$ is the anodic current density in the absence inorganic ions. The inhibitory efficiency improves as the concentration of inorganic ions increases (see Table 3). The sequence of increase in the inhibitors' inhibitory effectiveness is $WO_4^{2-} > MoO_4^{2-} > NO_2^-$.

Surface studies

The surface morphology caused by immersion in the corrosive solution (0.4 M Na_2SO_4 + 0.3 M $NaClO_4$) in the presence and absence of the compounds under consideration (ClO_4^-, WO_4^{2-}, MoO_4^{2-}, NO_2^- and NO_3^- ions, 0.03 M) were compared using the SEM methodology on nickel specimens.

The nickel specimens were subjected to (0.4 M Na_2SO_4 + 0.3 M $NaClO_4$) for 120 h around 30 degrees Celsius, and then they were taken from the solution and allowed to sit for an additional hour to dry before examination. According to Fig. 13a depicts the image of the untreated sample in the corrosive solution (0.4 M Na_2SO_4 + 0.3 M $NaClO_4$). In the absence of inhibitors, the large damaged regions, evident deteriorations, and pitting holes are visible.

In contrast, the microscope images of the tested nickel samples in the presence of the inhibitors, WO_4^{2-}, MoO_4^{2-}, NO_2^- and NO_3^-, in Fig. 13b–d, and e, respectively, showed highly effective corrosion inhibition efficiency as evidenced by the disappearance of deterioration areas, the disappearance of localized corrosion areas, and the fit (except NO_3^-).

The nickel surface was found to be very corrosive in the presence of NO_3^-ions (Fig. 13e). The present SEM results and the prior electrochemical technique results both show that the examined inhibitors (with the exception of NO_3^-) have effective corrosion control.

Conclusion

The current study investigates the anti-corrosion capabilities of various inorganic materials, such as WO_4^{2-}, MoO_4^{2-}, NO_2^- and NO_3^-, on nickel in Na_2SO_4 solution in the presence of perchlorate ions. Potentiodynamic curves show one dissolution peak (I), definitive passive, and transpassive state (II) regions. The data reveal that the anodic current density increase with increase in Na_2SO_4 solution concentration, potential scan rate (υ) and solution temperature. The progressive additions of $NaClO_4$ cause an increase in corrosion of nickel electrode and tend to breakdown the passive layer. The presence of the inorganic anions studied (Except NO_3^-) inhibits both anodic dissolution and pitting corrosion of nickel. The sequence of increase in the inhibitors' inhibitory effectiveness is $WO_4^{2-} > MoO_4^{2-} > NO_2^-$.

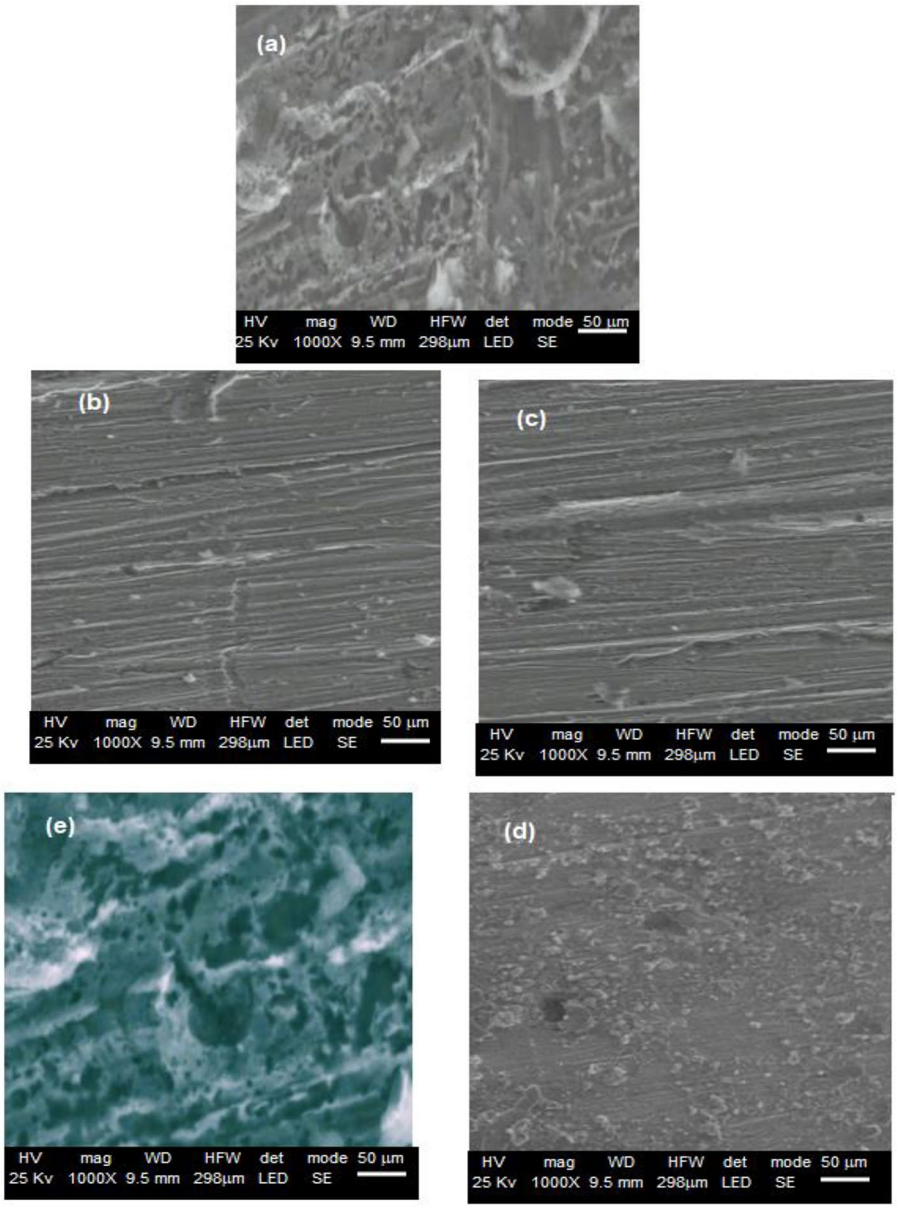

Figure 13. SEM images of Nickel samples in corrosive medium (0.4 M $NaSO_4$ + 0.3 M $NaClO_4$) (image (**a**)) and in the presence of the inhibitors, WO_4^{2-} (image (**b**)), MoO_4^{2-} (image (**c**)), NO_2^- (image (**d**)) and NO_3^- (image (**e**)). Immersion time: 120 h. Temperature: 30 °C.

Data availability

The datasets used and/or analysed during the current study available from the corresponding author on reasonable request.

Received: 22 October 2023; Accepted: 16 January 2024
Published online: 22 January 2024

References

1. Muñoza, A. G. & Schultze, J. W. Effects of NO_2^- on the corrosion of Ni in phosphate solutions. *Electrochim. Acta* **49**, 293 (2004).
2. Shi, X., Niu, L., Yang, G., Wang, H. & Jin, Z. Surface modification of nickel-based superalloy by electrochemical selective dissolution. *J. Alloys Compd.* **947**, 169628 (2023).
3. Petrauskas, A. V. *et al.* Potentiodynamic studies of the anodic behavior of Zn–Ni alloys electroplated from acetate-chloride baths. *Prot. Metals* **39**, 454–458 (2003).
4. Hummel, R. E., Smith, R. J. & Verink, E. D. The passivation of nickel in aqueous solutions—I. The identification of insoluble corrosion products on nickel electrodes using optical and ESCA techniques. *Corros. Sci.* **27**, 803–813 (1987).
5. Pan, Z., Luo, H., Zhao, Q., Cheng, H. & Li, X. Effect of Hf addition on microstructural evolution and corrosion behavior of nickel-based alloys in hydrochloric acid. *Corros. Sci.* **224**, 111507 (2023).

6. Bell, S., de Bruyn, M., Steinberg, T. & Will, G. Corrosion resistance of 625 nickel superalloy exposed to isothermal and thermal cycling conditions in a chloride/carbonate salt. *Solar Energy* **249**, 278–287 (2023).
7. Liu, H. *et al.* Metastable pitting corrosion behavior of laser powder bed fusion produced Ti6Al4V-Cu in 3.5% NaCl solution. *Corros. Sci.* **223**, 111452 (2023).
8. Li, W. & Luo, J. Pitting corrosion induced by the interaction between microstructures of iron-based alloy in chloride-containing solution. *J. Mater. Sci. Lett.* **21**, 1195–1198 (2002).
9. Hao, J.-Z. & Shi-Ai, Xu. Enhancement of the corrosion resistance of nickel-plated copper used for lithium-ion battery tabs with multilayer electroless coatings. *Mater. Today Commun.* **35**, 105924 (2023).
10. Ouarga, A. *et al.* Corrosion of iron and nickel based alloys in sulphuric acid: Challenges and prevention strategies. *J. Mater. Res. Technol.* **26**, 5105–5125 (2023).
11. Mobin, M. & Zehra, S. Chapter 13—Corrosion control by cathodic protection. In *Electrochemical and Analytical Techniques for Sustainable Corrosion Monitoring* (eds Aslam, J. *et al.*) 265–279 (Elsevier, 2023).
12. Zucchi, F., Fonsati, M. & Trabanelli, G. Corrosion and corrosion inhibition of nickel in $HClO_4$ solutions using the EQCM technique. *J. Appl. Electrochem.* **29**, 347–353 (1999).
13. Cheng, Y. F., Rairdan, B. R. & Luo, J. L. Features of electrochemical noise generated during pitting of inhibited A516–70 carbon steel in chloride solutions. *J. Appl. Electrochem.* **28**, 1371–1375 (1998).
14. Stoychev, D., Stefanov, P., Nicolova, D., Valov, I. & Marinova, T. S. Chemical composition and corrosion resistance of passive chromate films formed on stainless steels 316 L and 1.4301. *Mater. Chem. Phys.* **73**(2–3), 252–258 (2002).
15. Gassa, L. M., Vilche, J. R. & Arvía, A. J. A potentiodynamic study of anodic film formation on nickel in borate solutions. *J. Appl. Electrochem.* **13**, 135–145 (1983).
16. Smith, R. J., Hummel, R. E. & Ambrose, J. R. The passivation of nickel in aqueous solutions—II. An in situ investigation of the passivation of nickel using optical and electrochemical techniques. *Corros. Sci.* **27**(8), 815–826 (1987).
17. Pol, A., Sapakal, S., Khan, A. & Kadam, A. V. Synthesis of NiO thin film on 304-grade stainless steel substrate for oxygen evolution reaction. *Surf. Interfaces* **37**, 102706 (2023).
18. Mac Dougall, B., Mitchell, D. F. & Graham, M. J. The use of electrochemical and surface-analytical techniques to characterize passive oxide films on nickel. *Corrosion* **38**, 85–91 (1982).
19. MacDougall, B. & Graham, M. J. Effect of surface pretreatment on the galvanostatic oxidation of nickel. *Electrochim. Acta* **26**(6), 705–710 (1981).
20. Mac Dougall, B. & Cohen, M. Mechanism of the anodic oxidation of nickel. *J. Electrochem. Soc.* **123**, 1783 (1976).
21. Sato, N. & Okamoto, G. Electrochemical passivation of metals. In *Electrochemical Materials Science. Comprehensive Treatise of Electrochemistry* Vol. 4 (eds Bockris, J. O. *et al.*) (Springer, 1981).
22. Osterwald, J. & Uhlig, H. H. Anodic polarization and passivity of Ni and Ni-Cu alloys in sulfuric acid. *J. Electrochem. Soc.* **108**, 515 (1961).
23. Misra, R. D. K. & Burstein, G. T. The repassivation of nickel-copper alloys in sulphuric acid. *Corros. Sci.* **24**(4), 305–323 (1984).
24. Sun, H., Xinqiang, Wu. & Han, E.-H. Effects of temperature on the oxide film properties of 304 stainless steel in high temperature lithium borate buffer solution. *Corros. Sci.* **51**, 2840–2847 (2009).
25. Sato, N. & Okamoto, G. Anodic passivation of nickel in sulfuric acid solutions. *J. Electrochem. Soc* **110**, 605 (1963).
26. Láng, G., Ujvári, M. & Horányi, G. On the reduction of ClO_4^- ions in the course of metal dissolution in $HClO_4$ solutions. *Corros. Sci.* **45**(1), 1–5 (2003).
27. Bourkane, S., Gabrielli, C. & Keddam, M. Investigation of gold oxidation in sulphuric medium—II. Electrogravimetric transfer function technique. *Electrochim. Acta* **38**(14), 1827–1835 (1993).
28. Zucchi, F., Fonsati, M. & Trabanelli, G. Corrosion and corrosion inhibition of nickel in $HClO_4$ solutions using the EQCM technique. *J. Appl. Electrochem.* **28**, 441 (1998).
29. Abd El-Rehim, S. S., Abd El-Wahab, S. M., Fouad, E. E. & Hassan, H. H. Passivity and passivity breakdown of zinc anode in alkaline medium. *Mater. Corros.* **46**, 633 (1995).
30. Barbosa, M. R., Real, S. G., Vilche, J. R. & Arvia, A. J. Comparative potentiodynamic study of nickel in still and stirred sulfuric acid-potassium sulfate solutions in the 0.4–5.7 pH range. *J. Electrochem. Soc.* **135**, 1077 (1988).
31. Foad El-Sherbini, E. E., Abd-El-Wahab, S. M., Amin, M. A. & Deyab, M. A. Electrochemical behavior of tin in sodium borate solutions and the effect of halide ions and some inorganic inhibitors. *Corros. Sci.* **48**(8), 1885–1898 (2006).
32. Bockris, J. O. & Reddy, A. K. N. *Modern Electrochemistry* (McDonald, 1970).
33. Refaey, S. A. M. Inhibition of steel pitting corrosion in HCl by some inorganic anions. *Appl. Surf. Sci.* **240**, 396–404 (2005).
34. Refaey, S. S. & Abd El Rehim, S. S. Inhibition of chloride pitting corrosion of tin in alkaline and near neutral medium by some inorganic anions. *Electrochim. Acta* **42**, 667 (1996).
35. Hoar, T. P. The production and breakdown of the passivity of metals. *Corros. Sci.* **7**(6), 341–355 (1967).
36. Leckie, H. P. & Uhlig, H. H. Environmental factors affecting the critical potential for pitting in 18–8 stainless steel. *J. Electrochem. Soc.* **113**, 1262 (1966).
37. Foad El-Sherbini, E. *et al.* Effect of some polymeric materials on the corrosion behaviour of tin in succinic acid solution. *J. Appl. Electrochem.* **37**, 533–541 (2007).

Acknowledgements

The authors extend their appreciation to the Deanship of Scientific Research at King Khalid University for funding this work through small group Research Project under grant number (RGP. 1/336/44).

Author contributions

M.A.D., M.M.A., A.A.El-Z. reviewed the manuscript.

Competing interests

The authors declare no competing interests.

Additional information

Correspondence and requests for materials should be addressed to M.A.D.

Reprints and permissions information is available at www.nature.com/reprints.

Publisher's note Springer Nature remains neutral with regard to jurisdictional claims in published maps and institutional affiliations.